International Conference on Applied Energy 2019
Aug 12-15, 2019, Västerås, Sweden
Paper ID: 304

EFFECT OF TWO COMBINATION MODES OF DEPRESSURIZATION WITH WATER-GAS FLOW ON NATURAL GAS HYDRATE PRODUCTION

Mingjun Yang, Huiru Sun, Bingbing Chen, Yongchen Song*

Key Laboratory of Ocean Energy Utilization and Energy Conservation of Ministry of Education, Dalian University of Technology, Dalian, 116024, China

ABSTRACT

Natural gas hydrates (NGHs) production has aroused wide attention in recent years. Currently, the depressurization is regarded as the most effective method for hydrate production. However, there is still exist the insufficient driving force in depressurization anaphase. In this study, two modes of depressurization combined with water-gas flow was adopted to dissociated methane hydrate (MH). The results found that the depressurization can promote hydrate dissociation at first and optimized the water-gas flow environment by increasing permeability. And the water-gas flow will provide extra dissociation driving force by accelerating heat and mass transfer and increasing chemical potential difference. What's more, the mode of simultaneous implementation of depressurization and water-gas flow has a stronger promotion effect on hydrate production than the separate implementation of depressurization and water-gas flow.

Keywords: natural gas hydrate, depressurization, water flow erosion, water-gas flow, hydrate exploitation

NONMENCLATURE

Symbols	
S_{hi}	Initial MH saturation
V_w-V_g	Water flow rate-gas flow rate
t	Elapsed time for MH dissociation
P_d	Dissociation pressure
R_v	Average MH dissociation rate

1. INTRODUCTION

The energy consume is increasing continuously with the rapid industry development. It is necessary to found an alternative energy source for future. NGHs are abundantly distributed in permafrost and deep-water sediment, they are regard as the largest source of hydrocarbons and can provide plentiful natural gas resource [1] . Until now, depressurization [2], thermal stimulation [3], inhibitor injection [4] and CO_2 replacement [5] are proposed to recovery natural gas form hydrate sediment. Due to the lowest energy consumption, depressurization is considered as the most effective method to dissociate hydrate [6].

Currently, there are many investigations on hydrate dissociation characteristics induced by depressurization. Chong et al. [7]applied depressurization to recovery gas form a water saturated hydrate-bearing sediment, they found that a higher bottom hole pressure led to a slower production of water and gas. Sun et al. [8] proceeded a simulate experiment to product gas from hydrate reservoirs by using depressurization method, the results shown that the hydrate dissociation first appeared on the surface and outer layer of hydrate reservoirs than those of in inner. Li et al. [9] conducted depressurization experiment to dissociate hydrate and found that there will appear obvious increase of water extraction rate under the extremely low production pressure. Zhao et al. [10] investigated the influence of reservoir permeability on hydrate dissociation by depressurization method, and their results showed that there has a significant influence of surrounding ambient heat transfer on gas production in low permeability reservoirs.

However, the hydrate reformation, ice generation, and insufficient dissociation driving force in hydrate production anaphase significantly influent the gas

Selection and peer-review under responsibility of the scientific committee of the 11th Int. Conf. on Applied Energy (ICAE2019).

production rate. Due to the obvious effect of water flow erosion on promoting hydrate dissociation has been confirmed[11], while there are merely few studies to investigate the effect of water-gas two-phase on hydrate production. Therefore, the combination modes of depressurization with water-gas flow two-phase was proposed to improve hydrate dissociation driving force in this study.

2. PAPER STRUCTURE

2.1 Apparatus and materials

Fig.1 shows the schematic diagram of the experimental device, which mainly including a high-pressure vessel, three injection pumps, three thermostat baths, an MRI system, two pressure transducers, a differential pressure sensor and a data acquisition system. The MRI system can produce images of ^{1}H contained in liquids, so that it was used to monitor the variation of water distribution during MH formation and dissociation process. BZ-02 glass beads with a 35.4% porosity was used to simulate porous media. Methane gas with a 99.9% purity and deionized water was used in hydrate formation and dissociation process. Specific details of the experimental device can be found in the published paper by Chen et al. [11].

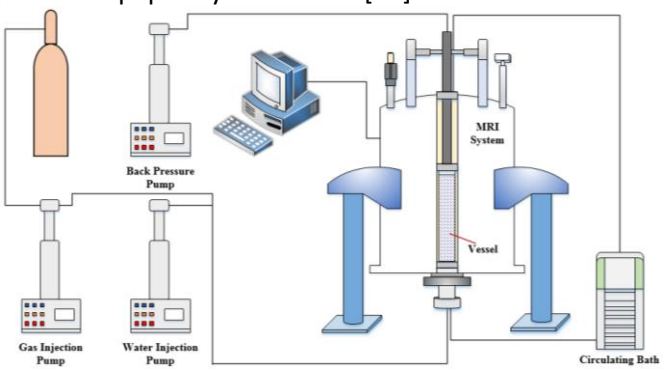

Fig.1 Schematic diagram of the experimental device

2.2 Experimental methods

The vessel filling with glass beads was placed into the MRI magnetic body. The free gas in vessel was discharged by a vacuum. Then, the deionized water was injected into the vessel to fully saturate porous media. Next, the gas was injected to displace deionized water in order to obtain the partially saturated porous media. After that, the vessel was pressured to 6000 kPa by gas injection and the vessel temperature was controlled at 274.15 K to start hydrate formation process. After the formation process completed, two modes were used for hydrate dissociation. For Case 1, the backpressure was set to 2000 kPa to dissociate MH at first, and then the water-gas flow started after 30 min until the hydrate dissociated completely. For Case 2, the depressurization and water-gas flow were used at the same time, in which the backpressure was also set to 2000 kPa and the water-gas flow rate was set to 5-1 ml·min^{-1}. The images of water distribution during hydrate dissociation process were recorded constantly by MRI system. The experimental parameters and results are shown in Table 1.

Table 1. Experimental parameters and results

Case	S_{hi}(%)	V_w- V_g (ml/min)	t(min)	P_d(kPa)	R_v(%)
1	23.44	5-1	102	2000	0.23
2	23.93	5-1	76	2000	0.31

3. RESULTS AND DISSOCIATION

In this study, two modes of depressurization combined with water-gas flow was adopted to dissociate MH. The temperature of flowing water and gas was controlled at 273.95 K, which eliminate the temperature change effect on hydrate dissociation. The water-gas flow rate was set to 5-1 ml·min^{-1} in Case 1 and 2, which was defined as water flow rate-gas flow rate.

3.1 MH dissociation by separate implementation of depressurization and water-gas flow

Fig.2 shows the water distribution variations during MH dissociation process by separate implementation of depressurization and water-gas flow (Case 1). The bright areas represent the liquid water, and the dark areas are considered as hydrate and less gas. As shown in Fig.2, the depressurization was solely used to dissociate hydrate at the period of 0-30min, in which the hydrate dissociation trend was form the both sides of the vessel to the center along radial direction caused by the heat transfer characteristic of surroundings. At 30 min, the whole image became wathet blue, which indicated the great mass of hydrate in vessel has been dissociated via depressurization. The reason was that the pressure of 2000 kPa provided a higher driving force for hydrate dissociation and induced the increase of water saturation in porous media. At the period of 30-102 min, the beginning of water-gas two-phase flow promoted the residua hydrate dissociation and further saturated the porous media, which made the image brighten obviously. This was because that the chemical potential difference between water-hydrate two phases can provide additional driving force to accelerate hydrate dissociation [11]. What's more, the water-gas flow also enhanced the heat and mass transfer process and avoided the ice generation.

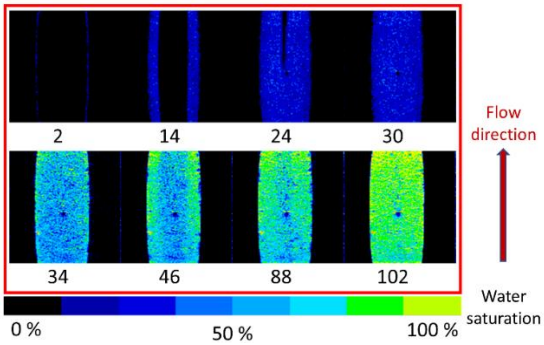

Fig.2 Water distribution variations during MH dissociation by separate implementation of depressurization and water-gas flow

Fig.3 shows the variations of MI and pressure during MH dissociation process by separate implementation of depressurization and water-gas flow. The MI variation will reflect the water saturation variation in porous media. As shown in Fig.3, the pore pressure always kept constant in hydrate dissociation process, which indicated the water and gas flow was smooth. In the MI variation curve, the points of A-B were corresponding to the pure depressurization stage, in which the MI gradually increased at first and then the upward trend slowed down and approached stability within 20-30 min. This phenomenon suggested that depressurization provided a large driving force to promote the hydrate dissociation in the initial stage. At the point of B, the water-gas flow with a 5-1 ml·min^{-1} flow rate started to replenish dissociation driving force. Because the higher flow rate will displace the hydrate-dissociated gas to backpressure pump quickly and increase the water saturation of porous media, so that the MI at the points of B-C rapidly rose to 1800 form 800. And at the points of C-D, the residual hydrate was dissociated by water-gas flow and resulted in the increase of MI gradually. When the hydrate dissociation process was finished, the MI will keep stable, corresponding to the points of D-E.

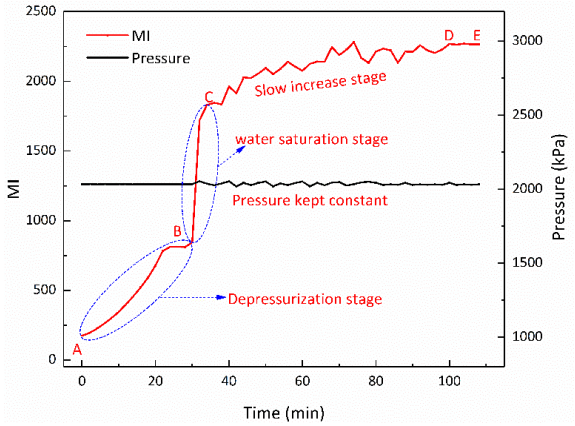

Fig.3 Variations of MI and pressure during MH dissociation by separate implementation of depressurization and water-gas flow

3.2 *MH dissociation by simultaneous implementation of depressurization and water-gas flow*

Fig.4 shows the variation of water distribution during hydrate dissociation by simultaneous implementation of depressurization and water-gas flow (Case 2). As shown in Fig.4, the hydrate was dissociated gradually and the images were changed to bright form dark. The duration of hydrate dissociation process (76 min) in Fig.4 was remarkable shorter than that in Fig.2 (102 min), and the average MH dissociation rate in Case 2 was 0.31 clearly higher than that of in Case 1 of 0.23 (shown in Table 1). That all indicated the simultaneous implementation of depressurization and water-gas flow has a stronger promotion effect on hydrate dissociation than the separate implementation of depressurization and water-gas flow. The reasons for this phenomenon are as follows. The depressurization caused the hydrate dissociation and released the pore space, which increased the water phase permeability and further optimized water-gas flow environment. In addition, the water-gas flow will facilitate hydrate dissociation and avoid ice generate by accelerating the heat and mass transfer process, further promote hydrate dissociation.

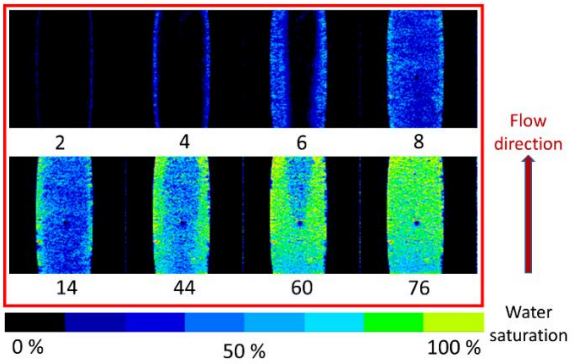

Fig.4 Water distribution variations during MH dissociation by simultaneous implementation of depressurization and water-gas flow

Fig.5 shows the variations of MI and pressure during MH dissociation by simultaneous implementation of depressurization and water-gas flow. As shown in Fig.5, there has a fast increase stage of MI at the points of A-B, which caused by amounts of hydrate dissociation under the joint effect of depressurization and water-gas flow. At the stage of B-C, the water-gas flow provided the main driving force for hydrate dissociation and the MI slowly increased. And the MI reached stability after the point of C that illustrated the completion of hydrate dissociation. Furthermore, compared to Fig. 3, the MI has a faster rising trend and a shorter time to reach stability in Fig.5, that also provided the mode of simultaneous

implementation of depressurization and water-gas flow was the most effective method for hydrate exploitation.

Considering the huge water source in accumulation area of gas hydrate and the water-gas flow in hydrate exploitation process, the combination mode of depressurization and water-gas two-phase flow was proposed. The main purpose of this study is to replenish hydrate dissociation driving force, avoid ice generation and hydrate reformation in hydrate exploitation process using depressurization. In the depressurization process, there exist a higher water-gas permeability with hydrate dissociation, and then the water-gas flow rate can be controlled by pressure difference between the drilling well and producing well. Therefore, the combination of depressurization and water-gas flow has an enormous potential for field hydrate production test. What's more, the optimal water-gas flow rate needs to be further determined, and the combination of depressurization and water-gas flow will be studied in the following work.

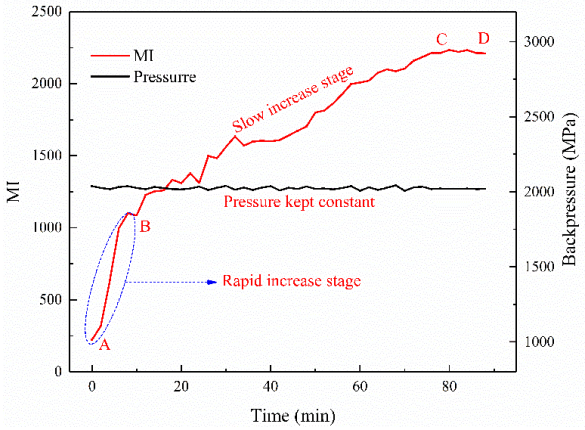

Fig.5 Variations of MI and pressure during MH dissociation by simultaneous implementation of depressurization and water-gas flow

4. CONCLUSION

In this study, two modes of depressurization combined with water-gas flow was used to recovery gas from hydrate sediment. According to the discussion above, the experimental results are summarized as follow: (1) Depressurization provided a higher initial driving force for hydrate dissociation and optimized water-gas flow environment. (2) Water-gas flow increased heat and mass transfer process and provided extra driving force for hydrate dissociation by increasing chemical potential difference. (3) The simultaneous implementation of depressurization and water-gas flow has a stronger promotion effect on hydrate dissociation than the separate implementation of depressurization and water-gas flow.

ACKNOWLEDGEMENT

This study was financially supported by grants from the National Natural Science Foundation of China (51436003, 51822603 and 51576025), the National Key Research and Development Plan of China (2017YFC0307303 and 2016YFC0304001), the Fok Ying-Tong Education Foundation for Young Teachers in Higher Education Institutions of China (161050) and the Fundamental Research Funds for the Central Universities of China (DUT18ZD403).

REFERENCE

[1] Loh M, Too JL, Faser S, Linga P, Khoo BC, Palmer A. Gas Production from Methane Hydrates in a Dual Wellbore System. Energy & Fuels. 2015;29:35-42.

[2] Chen B, Sun H, Zhou H, Yang M, Wang D. Effects of pressure and sea water flow on natural gas hydrate production characteristics in marine sediment. Applied Energy. 2019;238:274-83.

[3] Nair VC, Ramesh S, Ramadass GA, Sangwai JS. Influence of thermal stimulation on the methane hydrate dissociation in porous media under confined reservoir. Journal of Petroleum Science & Engineering. 2016;147:547-59.

[4] Li XS, Zhang Y, Li G, Chen ZY, Wu HJ. Experimental investigation into the production behavior of methane hydrate in porous sediment by depressurization with a novel three-dimensional cubic hydrate simulator. Energy & Fuels. 2011;25:4497-505.

[5] Brewer PG, Peltzer ET, Walz PM, Coward EK, Stern LA, Kirby SH, et al. Deep-sea field test of the CH_4 hydrate to CO_2 hydrate spontaneous conversion hypothesis. Energy & Fuels. 2014;28:7061-9.

[6] Zhao Jf, Liu D, Yang MJ, Song YC. Analysis of heat transfer effects on gas production from methane hydrate by depressurization. International Journal of Heat and Mass Transfer. 2014;77:529-41.

[7] Chong ZR, Yin ZY, Tan JHC, Linga P. Experimental investigations on energy recovery from water-saturated hydrate bearing sediments via depressurization approach. Applied Energy. 2017;204:1513-25.

[8] Sun JY, Ye YG, Liu CL, Zhang J. Experimental Study on Gas Production from Methane Hydrate Bearing Sand by Depressurization. Applied Mechanics and Materials. 2013;310:28-32.

[9] Li B, Li XS, Li G, Feng JC, Wang Y. Depressurization induced gas production from hydrate deposits with low gas saturation in a pilot-scale hydrate simulator. Applied Energy. 2014;129:274-86.

[10] Zhao J, Fan Z, Dong H, Yang Z, Song Y. Influence of reservoir permeability on methane hydrate dissociation by depressurization. International Journal of Heat and Mass Transfer. 2016;103:265-76.

[11] Chen BB, Yang MJ, Sun HR, Wang PF, Wang DY. Visualization study on the promotion of natural gas hydrate production by water flow erosion. Fuel. 2019;235:63-71.